MDPI

Article

Research on Gob-Side Entry Retaining Mining of Fully Mechanized Working Face in Steeply Inclined Coal Seam: A Case in Xinqiang Coal Mine

Xuming Zhou [1,2], Haotian Li [2,*], Xuelong Li [1,2,*], Jianwei Wang [3], Jingjing Meng [4], Mingze Li [2] and Chengwei Mei [2]

1   Mine Disaster Prevention and Control-Ministry of State Key Laboratory Breeding Base, Shandong University of Science and Technology, Qingdao 266590, China
2   College of Energy and Mining Engineering, Shandong University of Science and Technology, Qingdao 266590, China
3   Zhengmei Group, Engineering Technology Research Institute, Zhengzhou 450000, China
4   Department of Civil, Environmental and Natural Resources Engineering, Luleå University of Technology, 97187 Luleå, Sweden
*   Correspondence: 202183010042@sdust.edu.cn (H.L.); lixlcumt@126.com (X.L.)

Abstract: As a kind of non-coal pillar roadway support technique, gob-side entry retaining is of great significance to improve the production efficiency of a fully mechanized working face. However, the construction of the roadway is often subject to the surrounding rock conditions, the application is mainly concentrated in the nearly horizontal and gently inclined coal seam conditions, and the application in the steeply inclined coal seam conditions is relatively less. This paper is based on the gob-side entry retaining roadway construction of the 58# upper right 3# working face in the fifth district of Xinqiang Coal Mine, and describes the investigation in which we measured the advanced abutment stress, mining stress, and roof stress and analyzed the moving rule of roof. On this basis, in this work, we determined the filling parameters and process and investigated the filling effect from the perspective of the deformation of the filling body and the surrounding rock. The results show that the influence range of the advanced abutment stress in the working face is about 20~25 m, the stress in the upper part is intense, and stress in the middle and lower parts are relaxed. The setting load, the cycle-end resistance, and the time-weighted mean resistance at the upper end of working face along the direction of length are the largest, followed by the middle part, and the lower end is the minimum. When exploiting the steep inclined coal seam, the upper part of the working face is more active than the lower part, and the damaging range of overlaying strata is mainly in the upper part of the goaf. With this research, we established the filling mining process in steeply inclined coal seams and determined the relevant parameters. The gangue cement mortar filling can ensure the deformation of the filling body, the surrounding rock of the roadway is small in the process of roadway retention, and the stress of the filling body is also small, which ensure the successful retention of the roadway. This study verifies the possibility of repair-less exploitation and provides a reference for the popularization and application of the gob-side entry retaining technique in steep inclined coal seam.

Keywords: steeply inclined coal seam; gob-side entry retaining; roadside filling; surrounding rock control

1. Introduction

China has rich coal resources, accounting for about 40% of the world's production. For a long time to come, coal will be an irreplaceable dominant energy resource [1,2]. However, coal belongs to non-renewable energy. It has become an urgent problem to select an advanced mining technology to reduce the loss of coal resources [3]. As a kind

of non-coal pillar roadway support technique, gob-side entry retaining can reasonably develop existing coal resources and improve the recovery rate of coal resources [4,5]. Its research and promotion are significant to the development of the coal industry.

Although the gob-side entry retaining technique has been widely used worldwide, its application effect is often subject to the surrounding rock conditions of roadway retention, especially the stability of the roof [6–8], and the high cost also restricts its further promotion. To solve these problems, scholars have conducted a lot of research on the strata behavior, applicable conditions, reasonable support forms and new support materials. Through theoretical analysis and numerical simulation, Zhang et al. analyzed the roof cutting stress relief mechanism and the temporal and spatial evolution law of surrounding rock stress, and verified it in the field [9,10]. Bai et al. [11–13] used site investigation data, numerical simulation, and theoretical calculation to establish the dynamic mechanical model of the roof, and studied the roof bending deformation mode of the retained roadway. Fan et al. [14,15] used grouting cable to control roof cutting, built a surrounding rock support model composed of coal wall, support, and goaf gangue, and verified it in the working face. To analyze the subsidence law of roof after gob-side entry retaining in close coal seam, Liu et al. [16,17] calculated the stress distribution of the roof after mining, verified it by numerical simulation, and analyzed the failure process of the roadway roof under closed goaf, which provided guidance for gob-side entry retaining design with similar geological conditions. Chang et al. [18–20] combined numerical simulation and theoretical calculation to study the surrounding rock control effect of high-water fillings with different widths. Kumar et al. [21–23] put forward a construction method for roadway retention by using bag material and verified the feasibility using an indoor mechanical test based on the characteristics of thin coal seam mining. Li et al. [24,25] studied the key parameters of high-water filling material support when the retaining roadway in high-gas thin coal seams and studied the ground stress law by using roof displacement and filling body deformation.

In these studies, the stress state of surrounding rock and the interaction between support and surrounding rock were comprehensively analyzed. On this basis, scholars also carried out various explorations of gob-side entry retaining technology under different geological conditions and coal seam occurrence conditions and accumulated rich experience and lots of application cases. Qin et al. [26,27] used FLAC3D numerical simulation software to analyze the stress distribution law of gob-side entry retaining in thin coal seams and found that the horizontal stress gradually decreased with the advancement of the working face. He et al. [28–31] conducted directional fracturing of the roof with constant resistance and large deformation anchor cables and studied the reasonable support scheme under thick coal seam mining with numerical simulation and field observation. Guo et al. [32–34] studied the construction scheme of gob-side entry retaining technology under thick and hard roof conditions, proposed the pre-splitting blasting method, and conducted experiments on the site. Qi et al. [35–37] proposed a new scheme of gob-side entry retaining technology in three-soft coal seams based on the mechanical and numerical calculation model, including roadway expansion and large section roadway support, which provided theoretical guidance for construction under similar geological conditions. Based on site investigation and numerical analysis, Das et al. [38–40] analyzed the failure mechanism of the soft roof of a roadway in gently inclined coal seams and determined the bolt support parameters after working face advancement.

The above research mainly focuses on the geological conditions of the working face in the near-horizontal and gently inclined coal seam, which further fills the research gaps in the law of strata behavior, roadway support methods, and roadside filling techniques in gob-side entry retaining, and has been successfully applied onsite. However, there are still many problems in the application of gob-side entry retaining technology in medium-thick or thick coal seams with complex occurrence conditions, especially in large dip angle coal seams [41]. Some steeply inclined coal seams have not achieved the expected results in application, which limited the further application of the gob-side entry retaining technique.

The steeply inclined fully mechanized mining face in Xinqiang Coal Mine is rare in China. The research on the gob-side entry retaining technique in the working face needs to solve key problems, such as reasonable retention of the filling body, filling system and method, and stability of the filling body [42–44]. Related research can not only provide guarantees for safe and efficient production under the condition of steeply inclined coal seam, but also enrich and develop the gob-side entry retaining technology. Based on the gob-side entry retaining of the $58^{\#}$ upper right $3^{\#}$ working face in the fifth district of Xinqiang Coal Mine, we measured the advanced abutment stress and roof weighting, and analyzed the roof activity law. On this basis, we determined the filling parameters and process of the steeply inclined working face and investigated the filling effect from the perspective of the stress and deformation of the filling body and the surrounding rock. The theoretical and practical research in this paper can solve the problem of mine production and provide a demonstration for the popularization and application of the gob-side entry retaining technique under special working conditions.

2. Survey and Requirements in the Field

2.1. General Situation of Working Face

Xinqiang Coal Mine belongs to the Qitaihe Mining Bureau, using cross-cut development in a multi-level division of the vertical shaft method; the depth of the two horizons are −50 m and −300 m. There are, altogether, four production districts: $2^{\#}$, $3^{\#}$, $5^{\#}$, and $6^{\#}$. The location of the mine is shown in Figure 1. The fifth district is located in the eastern part of the mine. There are, altogether, three layers of coal seam, $54^{\#}$, $58^{\#}$, and $59^{\#}$, which are all coking coal and lean coal. The coal seam is roughly east-west strike and south dip. The dip angle is between $27°$ and $55°$ with an average of $45°$. With the deepening of mining, the dip angle of coal seam gradually increases. The fifth district $58^{\#}$ upper right $3^{\#}$ working face belongs to $2^{\#}$ mining horizon, and the depth is −156.83 m~−190 m, the strike length is 330 m, and the inclination length is 54~60 m. The immediate roof of the coal seam is 12.3 m siltstone, while the upper roof is 2.3 m medium sandstone and the floor is 17.0 m siltstone.
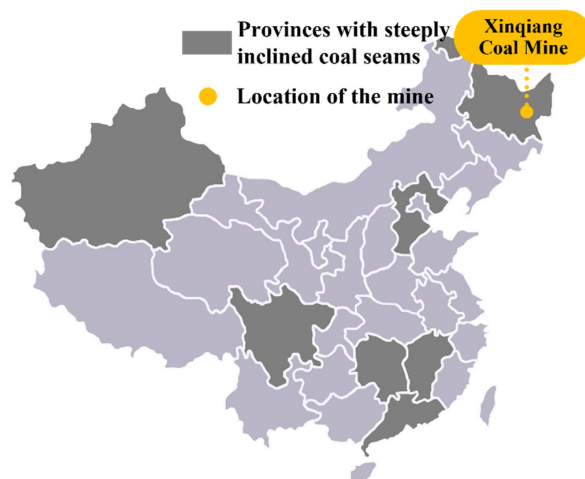

Figure 1. Distribution of steeply inclined coal seams and mine location.

The recoverable reserves of the fifth district $58^{\#}$ upper right $3^{\#}$ working face are 52,000 tons, adopted from the longwall backward mining method. The mining technology used a shearer drum to load coal, an armored face conveyor to transport coal, hydraulic supports to support the roof, and the total caving method to manage the roof. A MG2 × 125 (100)/580 (480) WD drum shearer and a ZY3600/12/28 shield hydraulic support was selected. The upper roadway belongs to $2^{\#}$ working face and the lower roadway is $3^{\#}$. The gob-side entry retaining roadway located in the $58^{\#}$ upper right $3^{\#}$ working face are shown in Figure 2. The average thickness of coal seam is 2.0 m, the height of the shearer is 1.25~2.58 m, the cutting depth of the drum is 0.8 m, and the effective support height is

1.2~2.8 m. The working face adopts the double drum one-way coal cutting method. The cycle footage is 0.8 m, and the mining height is 2.0 m, which is mined along the coal seam floor. The drum cuts triangular coal in the upward direction after feeds at the upper end, and then cuts coal in the downward direction. After the shearer sweeps the floating coal in the upward direction, the conveyor sequentially moves and supports.
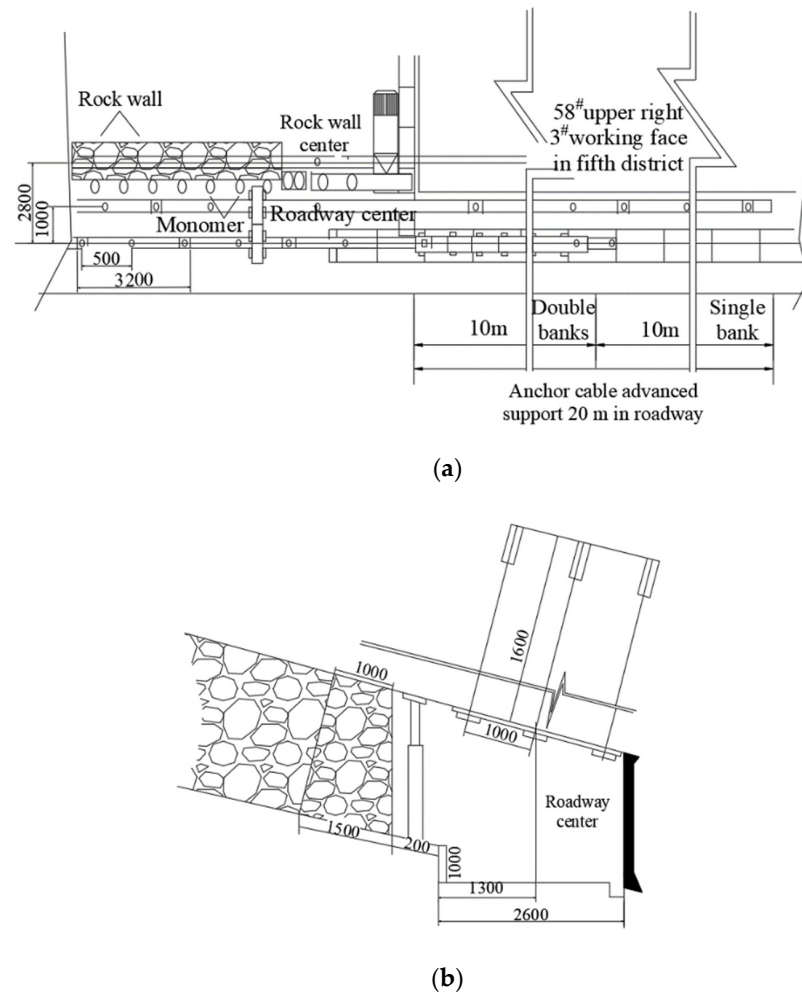

(a)

(b)

Figure 2. Views of gob-side entry retaining in 58[#] upper right 3[#] working face: (**a**) plan view; (**b**) sectional view.

2.2. Problems and Demands in the Field

Although the gob-side entry retaining technique has been valued and developed in China, it is restricted by the surrounding rock conditions and the stability of the roof is a key factor in construction effects [45]. The 58[#] upper right 3[#] working face in the fifth district of Xinqiang Coal Mine adopted the fully mechanized mining method; the advancing speed of the working face was fast, resulting in mining imbalance and a difficult replacement of the working face. To alleviate the production stress caused by mining imbalance, the gob-side entry retaining technology was adopted to retain the transportation roadway of the 3[#] working face as the return airway of the 4[#] working faces.

3. Roof Behavior in a Fully Mechanized Working Face in Steeply Inclined Coal Seam

3.1. Law of Advanced Abutment Stress

In the position of 100 m ahead of the working face on the coal side in the lower groove of the 58[#] upper right 3[#] working face in the fifth district, we drilled and installed a survey station. There were seven boreholes with depths of 2 m, 5 m, 8 m, 11 m, 14 m, 17 m, and 20 m. The height was about 1.5 m away from the roadway floor and the angle was

consistent with the coal seam dip angle (45°). The corresponding length of the stress sensor was installed into the borehole, numbered 1, 2, 3, 4, 5, 6, and 7. Among them, the No. 5 borehole stress sensor has oil leakage due to poor sealing during installation and the stress data has been zero. The other six borehole stress sensors have data, which can be used normally. The layout parameters of drilling and stress sensors are shown in Figure 3.
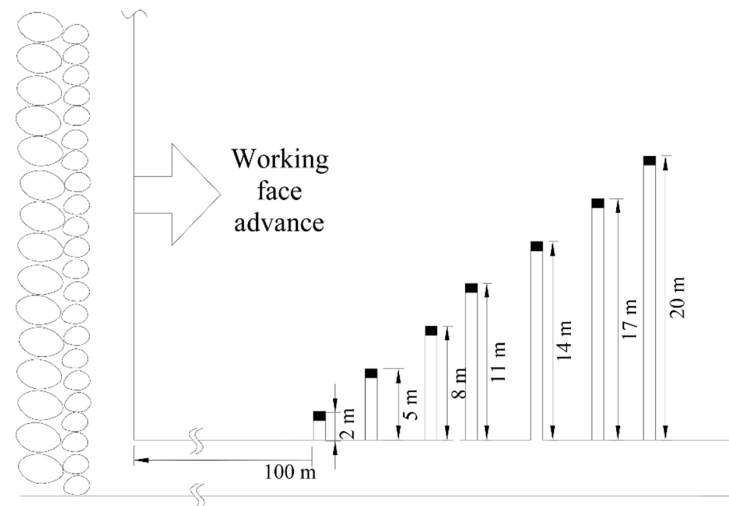

Figure 3. Schematic drawing of stress borehole measuring points.

The advanced abutment stress of the working face increases obviously from the initial stress at the position of about 6 m ahead of the working face, as shown in Figure 4. With the increase of the distance, the stress reaches the maximum at about 10 m from the working face, and the average peak stress is 14 MPa. After reaching the peak value, the stress begins to decrease, but is still higher than the initial stress; the influence continues to the position of 20~25 m from the working face and then restores to the initial stress value gradually. When the measuring point is about 25 m away from the working face, the stress sensor counting begins to change, indicating that the advanced abutment stress of the working face begins to affect the stress. The influence range of the advanced support stress of the working face is about 20~25 m, which is consistent with the empirical value of the end advanced support distance given in the field. Therefore, the end advanced support distance of the working face can meet the requirements of 25 m.
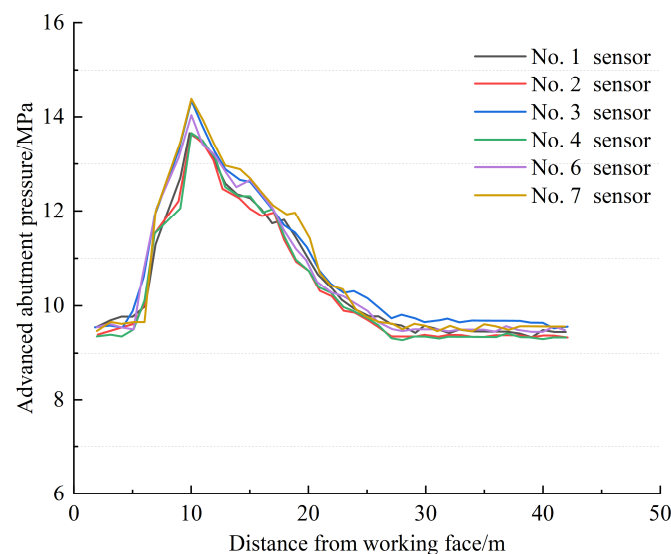

Figure 4. Distribution map of advanced abutment stress in working face.

3.2. Law of Rock Stress Activity

The measuring areas are arranged in the upper, middle, and lower parts along the face length direction of the 58# upper right 3# working face in the fifth district. We selected a support and installed stress gauges in each area to record the time-weighted mean resistance. The working face is a steeply inclined working face and the support quality of the hydraulic support in the working face is closely related to the three supports at the lower end. As a result, the support at the lower end was also selected and the digital stress gauge was installed. There are 60 hydraulic supports in the working face in total, and the stress gauges are installed on the 3#, 20#, and 36# supports to record the support resistance and the strata behavior. The position of the measuring points and the selected support are shown in Figure 5.
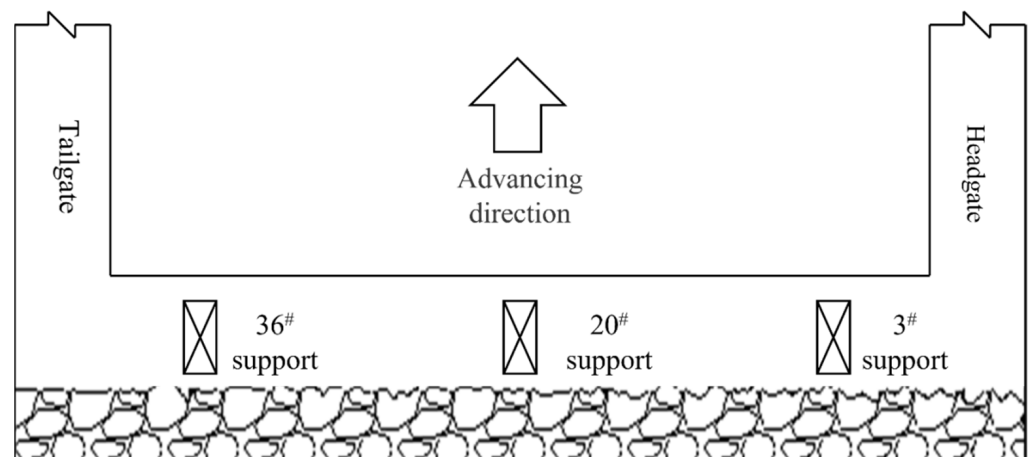

Figure 5. Layout drawing of rock stress measuring point.

The roof weighting data in each part of the working face are shown in Table 1, where K_m represents the end-of-cycle coefficient and K_t represents the time-weighted coefficient. According to Table 1, the 36# support weighted four times, the maximum stress step is 23.3 m, the minimum is 18.6 m, and the average is 20.5 m. The maximum influence range is 2.8 m, the minimum is 2.1 m, and the average is 2.35 m, and the dynamic load coefficients during the weighting period are $K_m = 1.29$ and $K_t = 1.28$. Therefore, the stress strength in the upper part of the working surface (36# support) is intense. The 20# support weighted four times, the maximum stress step is 25.6 m, the minimum is 21.6 m, and the average is 23.6 m. The maximum influence range is 3 m, the minimum is 1.2 m, and the average is 2.375 m, and the dynamic load coefficients during the weighting period are $K_m = 1.21$ and $K_t = 1.22$. Therefore, the stress strength in central part of working surface (20# support) is mild. The measurement shows that the 3# support weighted three times, the maximum stress step is 34.6 m, the minimum is 30.4 m, and the average is 32.4 m. The maximum influence range is 3.2 m, the minimum is 2.4 m, and the average is 2.8 m, and the dynamic load coefficients during the weighting period are $K_m = 1.06$ and $K_t = 1.04$. Therefore, the stress strength in the lower part of the working surface (3# support) is mild. At the same time, it can be seen from Table 1 that the dynamic load coefficients of the upper, middle, and lower roof weighting are 1.28, 1.21, and 1.04, respectively, which are values far less than the dynamic load coefficient of gently inclined coal seam. The average periodic weighting step distance of the upper, middle, and lower parts of the working face is 20.5 m, 23.6 m, and 32.4 m, respectively, which is much larger than that of gently inclined coal seam. The roof stress behavior of coal seam in the working face is mild and the periodic weighting is not obvious.

The roof stress distribution along the face length direction of the steeply inclined fully mechanized working face is different when affected by the mining method, the coal and rock occurrence conditions and support quality, and especially the dip angle of coal

seam [46,47]. The stress distribution in the long direction of the working face during the periodic weighting and non-periodic weighting is shown in Figure 6.

Table 1. Roof weighting data in working face.

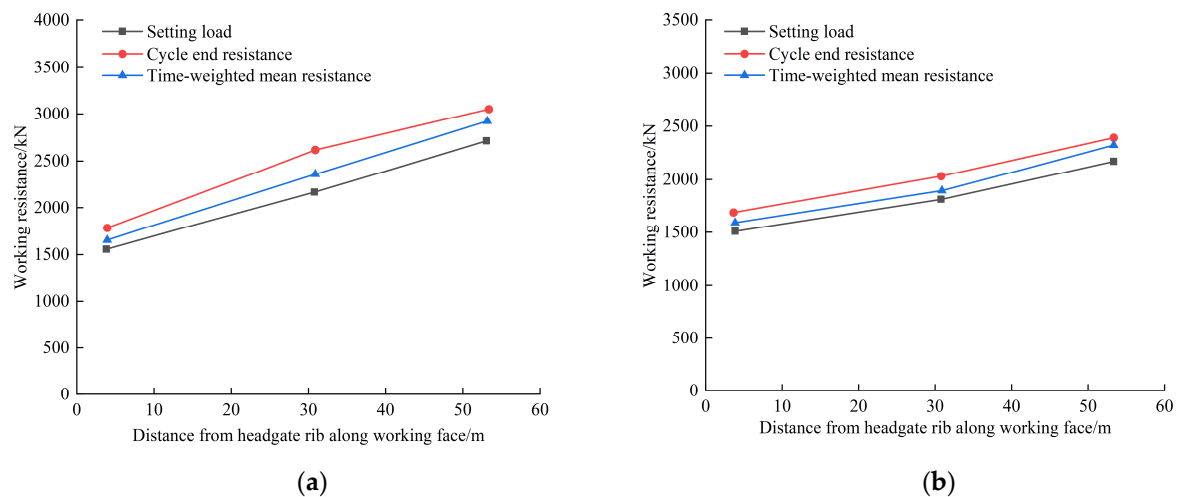| Support Number	Number of Weighting	Step Distance(m)	Range of Influence (m)	Dynamic Load Coefficient	
				K_m	K_t
36	4	20.5	2.35	1.29	1.28
20	4	23.6	2.37	1.22	1.21
3	3	32.4	2.8	1.06	1.04

(**a**)

(**b**)

Figure 6. Distribution of roof stress along the length direction of working face: (**a**) weighting period; (**b**) non-weighting period.

It can be seen in Figure 6a that, during the weighting period, the working resistance in the lower end of the working face is the lowest, the setting load P_o is only 1557 kN, the cycle-end resistance P_m is 1782 kN, and the time-weighted mean resistance P_t is 1653 kN. With the increase of distance, the working resistance of the support in the middle of the working face also increases, with an increase of 610 kN, 834 kN, and 707 kN, respectively. With the further increase of the distance from the headgate, the setting load, cycle-end resistance, and time-weighted mean resistance in the end of the working face are the maximum, which are 2713 kN, 3050 kN, and 2922 kN, respectively. During the weighting period, the average setting load of the three supports is 2145 kN, which is 69.39% of the rated setting load (3092 kN). The average cycle-end resistance is 2482 kN, which is 68.94% of the rated working resistance (3600 kN). Therefore, the design makes full use of the rated bearing capacity of the support while ensuring reliability. It is shown in Figure 6b that, during the non-weighting period, the working resistance also shows a trend of increasing with distance. At the lower end of the working face, the setting load, the cycle-end resistance and the time-weighted mean resistance are all minimum values, which are 1506 kN, 1686 kN, and 1589 kN, respectively. With the increase of the distance from the headgate, the working resistance increases slightly, reaching 1811 kN, 2032 kN, and 1894 kN in the middle of the working face. The maximum values of setting load, cycle-end resistance, and time-weighted mean resistance appear at the upper end of the working face, and the resistance values are 2170 kN, 2391 kN, and 2322 kN, respectively, during the same stress period.

3.3. Characteristics of Roof Weighting

The gravity effect of overlying strata in steeply inclined coal seams is different from that in nearly horizontal and gently inclined coal seam, resulting in different roof weighting characteristics.

(1) The roof behavior of steeply inclined coal seam is mild; periodic weighting is not obvious. The weighting strength is significantly lower than that of gently inclined coal seam, while the weighting step distance is significantly larger than that of gently inclined coal seam. The reason is that the component force of the gravity action of overlying strata on the roof of coal seam is much smaller than that of gently inclined coal seam. This also leads to hydraulic support stress in the steeply inclined coal seam working face being small; support performance can meet the requirements, so the support design should mainly consider the support equipment anti-skidding.

(2) The periodic weighting difference of each position in the face length direction of steeply inclined coal seam is large, but the overall weighting difference of the working face is not large, especially the upper and central parts. In comparison, the periodic weighting at the upper end of the working face is stronger than that at the middle of the working face, while the periodic weighting at the middle is stronger than that at the bottom of the working face. The reason is that the dip angle of coal seam is much larger than the natural repose angle of coal and rock mass. When the immediate roof is broken, the weak immediate roof rock mass in the upper part of the goaf rolls down to the lower part under the action of self-weight, forms a state of full enrichment in the top, semi-enrichment in the middle, and hanging in the bottom in the length direction of the working face. Therefore, the periodic weighting step distance and dynamic load coefficient are inconsistent in the length direction of the working face.

4. Gob-Side Entry Retaining and Backfilling Process in Steeply Inclined Coal Seam

4.1. Advantages of the Gob-Side Entry Retaining Technique

The gob-side entry retaining technique has the following advantages for the 58[#] upper right 3[#] working face in the fifth district of Xinqiang Coal Mine:

(1) The gob-side roadway is synchronously filled and maintained with the advance of the working face, which ensures the normal transportation of the material, raw coal, and fresh air of the working face. It is also conducive to the safe production of the mine.

(2) The roadways retained along the goaf can be used as the flat roadway in the next working face, which can save the tunneling cost of the roadway and avoid continuous tension and mining imbalance.

(3) The district sublevel coal pillar between working faces is omitted, which greatly improves the recovery rate of coal resources.

4.2. Determination of Filling Parameters

The haulage roadway of the working face is excavated along the coal seam roof. In the process of roadside filling, the retention roadway is strengthened by the support. The roof and floor of the roadway in the goaf side are punched with anchor cables to maintain the stability of the roadside filling body. To prevent the slurry from overflowing into the roadway due to the fluidity of the slurry during the initial grouting of the filling material, the wooden plate is added between the anchor cables and the filling body. The personnel have difficulty entering the goaf side, so the slurry flows naturally in the early stage of backfilling and stops grouting when the size of the filling body is qualified. The physical properties of the slurry determine the natural resting angle of the filling body and the plane section of the filling body is finally trapezoidal, as shown in Figure 7.

According to the geological conditions of the coal seam in the mine, the total stress of overlying strata on the filling zone can be directly calculated according to the multiple rock weight method (estimation method) P_t [48]. The formula is as follows:

$$P_t = ngS\gamma M \cos\alpha \tag{1}$$

The working resistance of filling body P_T is:

$$P_T = \sigma S_t \tag{2}$$

The strength requirements of roadside filling body is:

$$P_T \geq P_t \tag{3}$$

The filling body will not be damaged, the roadway retained along the goaf can be completely preserved [49]. Three formulas stand together and can be derived that:

$$S_t \geq ngS\gamma M \cos\alpha / \sigma \tag{4}$$

In the formula, S_t is the area supported by filling body; n is the rock weight multiple according to the medium stability below the roof consideration, generally taken as 6~8; g is the gravitational acceleration, S is the roof area supported by filling body, which is $S = ab$; a is the length of filling body along the roadway direction, b is the width of the roof supported by the filling body, γ is the density of roof strata, M is the cutting height; α is the dip angle of coal seam, taken as an average of 45°; and σ is the compression of the filling body.

The shape of the filling body is trapezoidal due to the geological conditions of roadside filling in steeply inclined coal seam, so the sum of the upper and lower boundaries of the trapezoid determines that the cross-sectional area of the filling body should not be less than 6 m. Considering that the filling body is incompressible, the filling body supports the overlying strata other than the immediate roof and the main roof. For safety purposes, the designed average width of the filling body is 3 m, as shown in Figure 8.
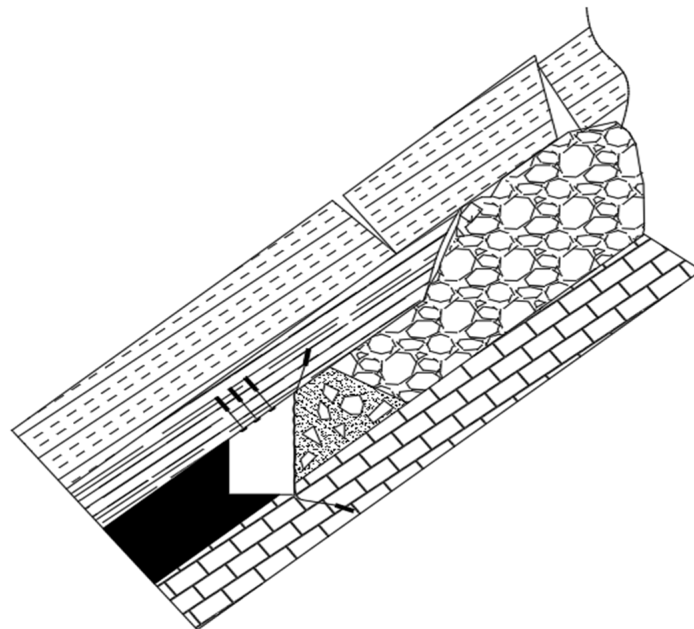

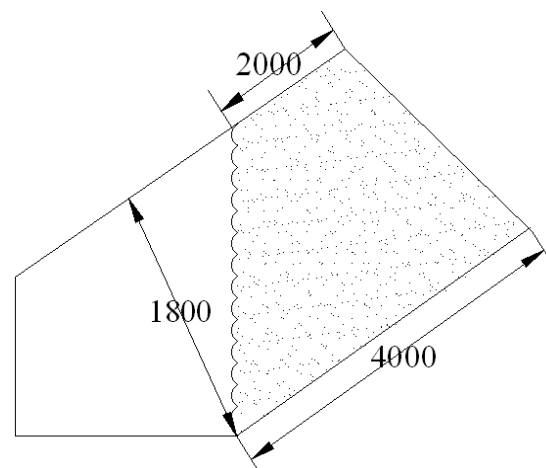**Figure 7.** Trapezoid filling body and roof structure.

Figure 8. Geometric dimensions of filling body (mm).

4.3. Process of Backfilling

(1)   Processing and transportation of filling materials

After drying the sand, stone, and fly ash in the ground workshop, put the materials into the mixer according to the prescribed ratio and mix evenly. Then, load the mixture into the woven bag and transport it to the underground working surface by the mine truck.

(2)   Filling and pumping of filling materials

According to the advancing time of the working face, each advancing cycle (0.8 m) of the working face should fill once. The filling pump is used to transport the uniformly stirred material through the pipeline into the filling space isolated by the baffle.

(3)   Filling space

Clean the floating coal after the downward cutting of the cutting coal machine in the working face. The support is pushed forward from the bottom to the top, the fourth support that is close to the upper side of the filling body of the working face is retained, and the filling space is formed behind the bent support. The filling bag and the filling partition are laid in the filling space to resist the impact of a small amount of gangue on the goaf side. At the same time, the trapezoidal partition is laid behind the shield beam of the lower end row head frame, the rectangular partition is erected on the roadway wall, and the single pillar is initially blocked. The filling space surrounded by roadway wall, unmoved support (fourth support), bent shield beam, and filling body are shown in Figure 9. Subsequently, the outlet of the filling pipeline enters the filling port of the filling partition and the filling material is injected into the space. At the same time, thick wood plates are placed in advance above the filling bag to buffer the roof subsidence and prevent the roof subsidence of the retaining wall from crushing the wall before it reaches the predetermined strength.
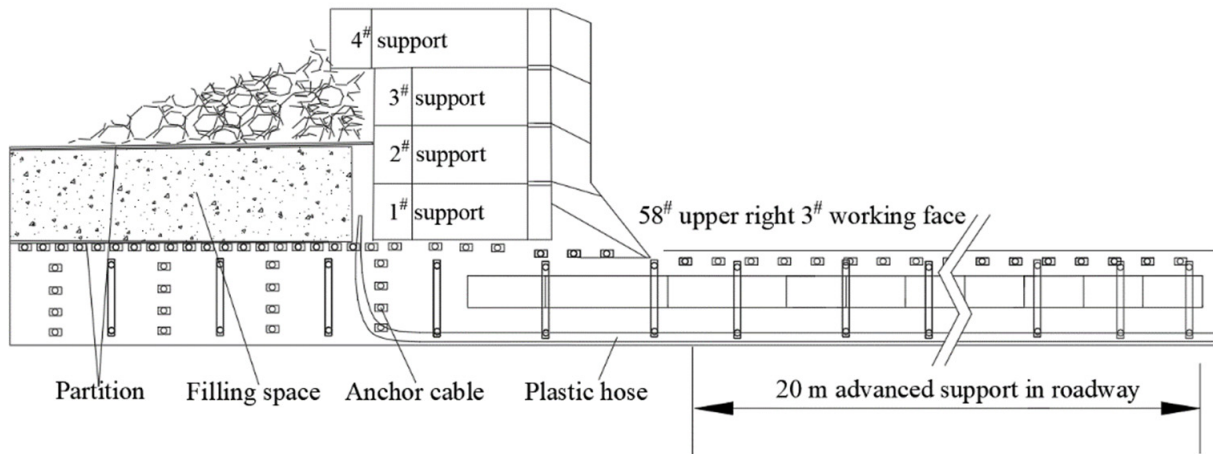
Figure 9. Schematic drawing of filling space.

(4)   Complete filling work

At the end of filling, the filling material is no longer filled in the pump, the material in the pipe should be pushed clean with plastic balls, and the full-length pipe should be washed once with water to prevent solidification and blockage of filling materials in the pipe. At the same time, the next filling preparation work should be done. The filling pump is arranged in the transportation roadway. When the working face is pushed over, the filling pump does not need to be moved because it is in the retained roadway, and the filling pipeline only needs to be extended outward.

The sequence and process of gob-side entry retaining in Xinqiang Mine are shown in Figure 10.
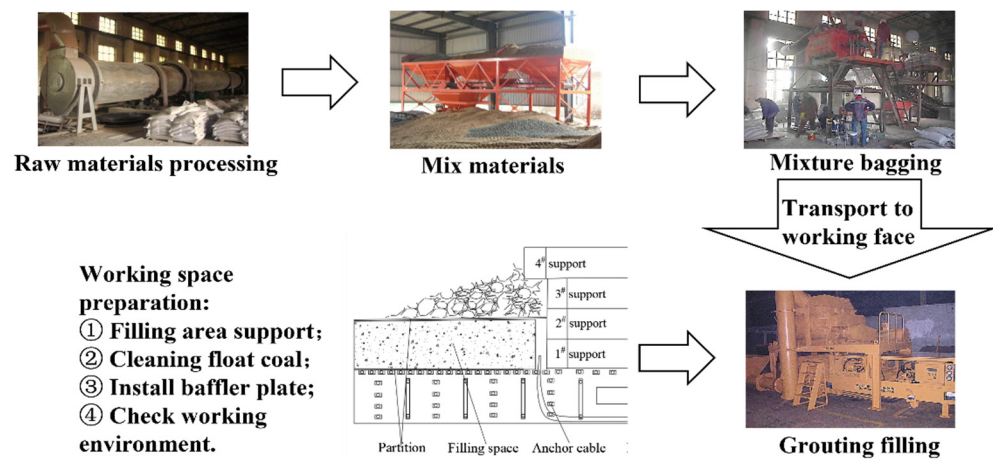
Figure 10. Process of backfilling.

4.4. Filling Effect Monitoring

To examine the filling effect and the strength and deformation characteristics of the roadside filling body, we installed displacement sensors (Figure 11a), borehole stress sensors (Figure 11b), and surrounding rock deformation sensors (Figure 11c) during the process of roadside filling to record experimental data and investigate whether the filling body meets the strength and deformation requirements. The letters A to F in the figures represent sensors in different locations, and the letters with circles represent the corresponding indicators.
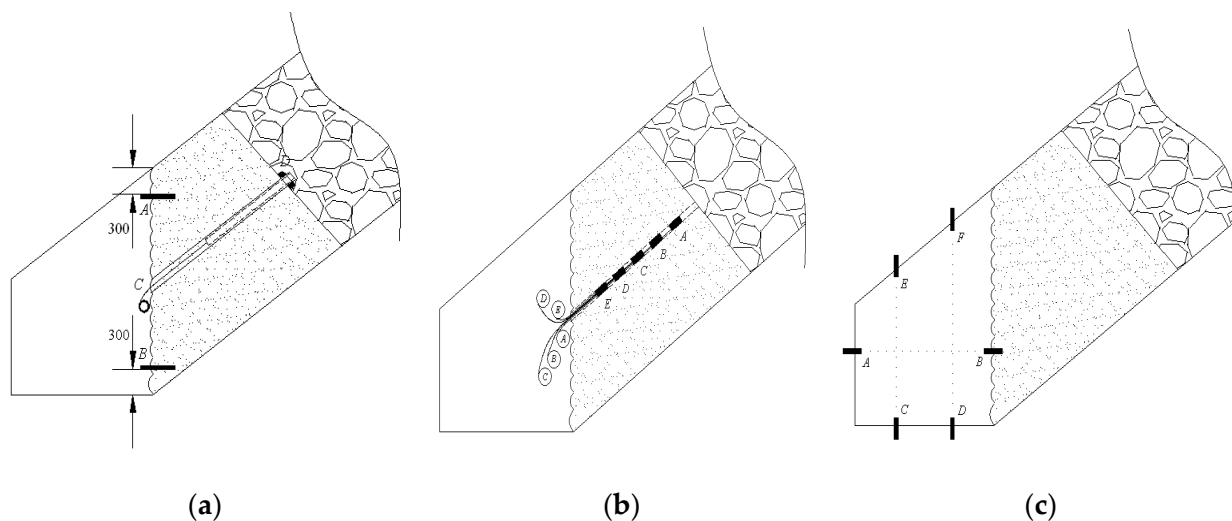

(a)　　　　　　　　　　　　　　(b)　　　　　　　　　　　　　　(c)

Figure 11. Layout drawing of sensors: (**a**) displacement sensors; (**b**) borehole stress sensors; (**c**) surrounding rock deformation sensors.

5. Investigation of Filling Effect

5.1. Deformation Characteristics of Filling Body

The stress sensors are embedded in the filling body after the roadside filling. The transverse and longitudinal deformation of the filling body obtained by a period of testing is shown in Figure 12.

The deformation of the filling body can be roughly divided into five stages. In the initial construction stage of the filling body, the distance from the working face is generally about 10 m and the deformation of the roadway roof is small. The filling body cannot be actively bear stress and the deformation in two directions is almost zero. In the range of 10~20 m away from the working face, the rock stress begins to appear; the amount and ratio

of the roof-to-floor convergence gradually increase and the filling body gradually begins to actively bear stress. Due to the high strength of the cement mortar filling body in the initial solidification stage, the roof subsidence is not large at this stage. In the distance of about 20~40 m from the working face, the overlaying strata of the roof moves violently and the roof-to-floor convergence further increases. The vertical and horizontal deformation of the filling body can reach 57 mm and 31 mm. In the range of 40~80 m away from the working face, the activity of roadway roof strata gradually eases, the deformation of filling body gradually stabilizes, and the longitudinal deformation generally does not exceed 100 mm. At about 80 m away from the working face, the filling body becomes stable and there is basically no vertical and horizontal deformation.
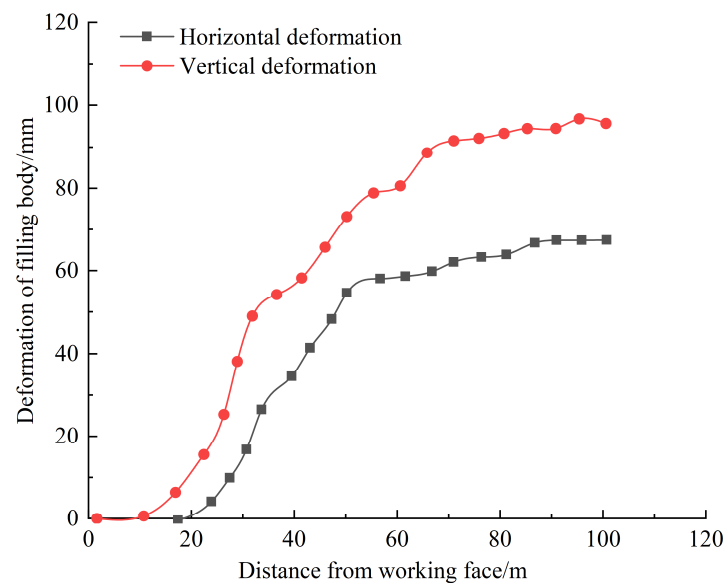

Figure 12. Deformation curves of filling body in different stages.

5.2. Stress Characteristics of the Filling Body

The borehole stress sensors were installed in the roadside backfills in different distances from the working face to measure the loads borne by the backfills at different locations in the backfills, as shown in Figure 13.
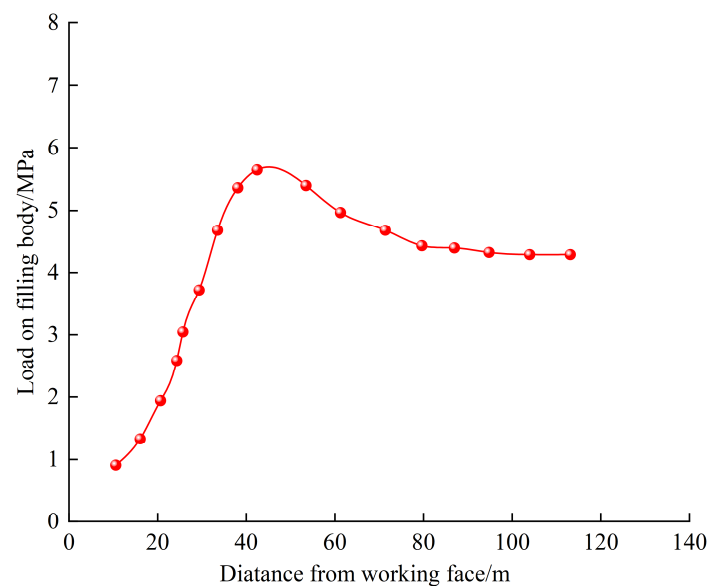

Figure 13. Load variation curve in filling body.

With the increase of the distance from the working face, the trend of the load in the roadside filling body can be roughly divided into three stages. At about 10 m from the working face, the displacement of the roadway roof increases, and the filling body gradually begins to bear a certain load. Subsequently, the load shows an increasing trend with the increase of distance. The fastest increase is in the range of 20~40 m. At about 40 m from the working face, the filling body reaches the ultimate strength, about 6 MPa. In the range of 40~80 m from the working face, the filling body gradually tends toward a plastic yield state under the action of a severe deformation of the roadway roof and the bearing capacity reduces as the load reduces. The deformation of the roadway roof tends to be stable and the load distribution in the roadside filling body tends to be stable and no longer decreases in the range outside of 80 m.

5.3. Deformation Characteristics of Roadway-Surrounding Rock

When the working face advances, the roof and floor of the retained roadway are always in the state of spatial motion. The activity intensity of the roadway roof and floor is related to the distance from the working face, which leads to a different roof convergence. Figure 14a shows the relationship between the displacement of the roof and floor of the retained roadway behind the working face and the distance from the working face. Figure 14b shows the relationship between the displacement of the two sides of the reserved roadway and the distance from the working face.
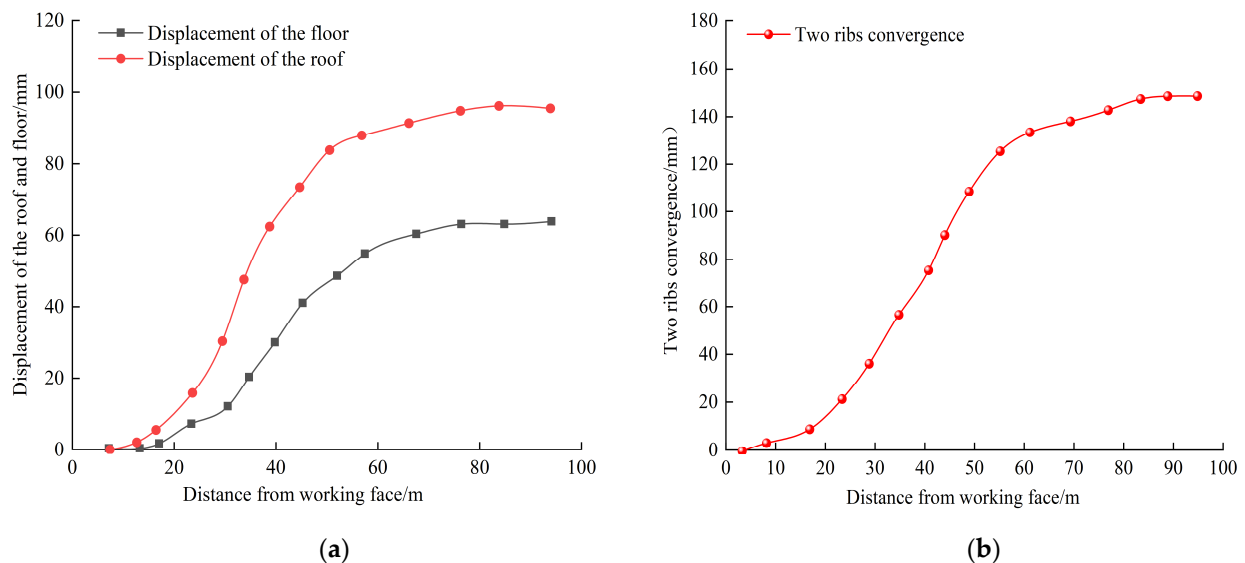

(**a**)   (**b**)

Figure 14. Variation curve of roadway-surrounding rock: (**a**) roof-to-floor convergence; (**b**) two ribs convergence.

It can be seen from the measurement results that the displacement of the roof-to-floor convergence and two ribs of the retained roadway slightly changes within the range of 10~20 m from the working face. In the range of 20~50 m from the working face, the roof-to-floor convergence and the two ribs' displacement increase rapidly, and the displacement is approximately linear with the length of the working face. At about 50 m from the working face, the sum of the two ribs' displacement reaches about 116 mm. In the range of 50~80 m from the working face, due to the stable motion state of the surrounding rock, the displacement of the two ribs of the roadway numerically increases, but the increase rate is less than the previous stage. At about 80 m away from the working face, the surrounding rock movement becomes stable and the roadside filling body bears a stable load. The roof-to-floor convergence is less than 100 mm, and the displacement of the two ribs is not more than 140 mm.

6. Conclusions

To study the gob-side entry retaining technique in steeply inclined coal seam, we measured the advanced abutment stress, mining stress, and roof stress, and analyzed the moving rule of roof based on the gob-side entry retaining roadway construction of the 58[#] upper right 3[#] working face in the fifth district of Xinqiang Coal Mine. On this basis, in this work, we determined the filling parameters and process of the steeply inclined working face and investigated the filling effect from the perspective of the stress and deformation of the filling body and the surrounding rock. The results show that:

(1) The influence range of the advanced abutment stress of the working face is about 20~25 m, which is consistent with the empirical value of the advanced support distance in the field. The stress intensity in the upper part of the working face is intense; the stress intensity in the middle and lower part of the working face is mild.

(2) During the period of periodic weighting or not, the setting load, the cycle-end resistance, and the time-weighted mean resistance at the upper end of the working face along the direction of length are the largest, followed by the middle part, and the lower end is the minimum. The increase is greater during the weighting period than during the non-stress period.

(3) The overlaying strata in the upper part of the working face is more active than the lower part when mining steeply inclined coal seam. The range of rock failure is mainly in the upper part of the goaf, the upper roof has a tensile fracture due to sliding instability, and the lower part is unevenly filled by falling gangue. Due to the rotary instability stress on the filled gangue, the floor heave phenomenon is obvious.

(4) The filling mining process of steeply inclined coal seam is established. The multiple estimation method was used to determine and calculate the relevant parameters of trapezoidal backfill and the field observation was carried out. The roadside filling body constructed by gangue cement mortar material has a fast setting speed and strong bearing capacity. After filling, the deformation of the filling body and the roadway-surrounding rock is small and the stress of the filling body is small, indicating that the filling effect is good. This study verifies the possibility of repair-less exploitation and provides reference for mines with the same conditions.

Author Contributions: X.Z., H.L. and X.L. proposed the research. J.W. and J.M. prepared figures and tables, and interpreted the structural data. M.L. and C.M. developed the main ideas. All co-authors actively contributed to the manuscript with comments, ideas, and suggestions. All authors have read and agreed to the published version of the manuscript.

Institutional Review Board Statement: Not applicable.

Informed Consent Statement: Not applicable.

Data Availability Statement: The datasets used and/or analyzed during the current study are available from the corresponding author on reasonable request.

Conflicts of Interest: The authors declare no potential conflict of interest with respect to the research, authorship, and/or publication of this paper.

References

1. Mohr, S.H.; Evans, G.M. Forecasting coal production until 2100. *Fuel* **2009**, *88*, 2059–2067. [CrossRef]
2. Bai, X.F.; Ding, H.; Lian, J.J.; Ma, D.; Yang, X.Y.; Sun, N.X.; Xue, W.L.; Chang, Y.J. Coal production in China: Past, present, and future projections. *Int. Geol. Rev.* **2018**, *60*, 535–547. [CrossRef]

3. Wu, R.; He, Q.Y.; Oh, J.; Li, Z.C.; Zhang, C.G. A new gob-side entry layout method for two-entry longwall systems. *Energies* **2018**, *11*, 2084. [CrossRef]

4. Wang, Q.; He, M.C.; Yang, J.; Gao, H.K.; Jiang, B.; Yu, H.C. Study of a no-pillar mining technique with automatically formed gob-side entry retaining for longwall mining in coal mines. *Int. J. Rock. Mech. Min.* **2018**, *110*, 1–8. [CrossRef]

5. Ma, Z.M.; Wang, J.; He, M.C.; Gao, Y.B.; Hu, J.Z.; Wang, Q. Key technologies and application test of an innovative noncoal pillar mining approach: A case study. *Energies* **2018**, *11*, 2853. [CrossRef]

6. Kan, J.G.; Zhang, N.; Wu, J.K.; Wu, H. Effect of main roofs fracture position on the secondary gob-side entry retaining stability. *Disaster Adv.* **2013**, *6*, 189–199.

7. Zhou, X.M.; Wang, S.; Li, X.L. Research on theory and technology of floor heave control in semi-coal rock roadway: Taking Longhu coal mine in Qitaihe mining area as an example. *Lithosphere* **2022**, *11*, 3810988. [CrossRef]

8. Luan, H.J.; Jiang, Y.J.; Zhou, L.J.; Lin, H.L. Stability control and quick retaining technology of gob-side entry: A case study. *Adv. Civ. Eng.* **2018**, *2018*, 7357320. [CrossRef]

9. Zhang, Y.; Xu, H.C.; Song, P.; Sun, X.M.; He, M.C.; Guo, Z.B. Stress evolution law of surrounding rock with gob-side entry retaining by roof cutting and stress release in composite roof. *Adv. Mater. Sci. Eng.* **2020**, *2020*, 1961680. [CrossRef]

10. Islavath, S.R.; Deb, D.; Kumar, H. Numerical analysis of a longwall mining cycle and development of a composite longwall index. *Int. J. Rock. Mech. Min.* **2016**, *89*, 43–54. [CrossRef]

11. Bai, J.B.; Shen, W.L.; Guo, G.L.; Wang, X.Y.; Yu, Y. Roof deformation, failure characteristics, and preventive techniques of gob-side entry driving heading adjacent to the advancing working face. *Rock. Mech. Rock. Eng.* **2015**, *48*, 2447–2458. [CrossRef]

12. Guo, P.F.; Zhao, Y.X.; Yuan, Y.D.; Ye, K.K.; Zhang, H.J.; Gaol, Q. Gob-side entry stability analysis by global-finite and local-discrete modeling approach. *Geomech. Eng.* **2021**, *27*, 391–404.

13. Liu, S.M.; Li, X.L.; Wang, D.K.; Zhang, D.M. Investigations on the mechanism of the microstructural evolution of different coal ranks under liquid nitrogen cold soaking. *Energ. Source Part A* **2020**, *10*, 1–17. [CrossRef]

14. Fan, D.Y.; Liu, X.S.; Tan, Y.L.; Yan, L.; Song, S.L.; Ning, J.G. An innovative approach for gob-side entry retaining in deep coal mines: A case study. *Energy Sci. Eng.* **2019**, *7*, 2321–2335. [CrossRef]

15. Kumar, R.; Mishra, A.K.; Singh, A.K.; Ram, S.; Singh, R. Depillaring of total thickness of a thick coal seam in single lift using cable bolts: A case study. *Int. J. Min. Sci. Technol.* **2016**, *26*, 223–233. [CrossRef]

16. Liu, H.Y.; Zhang, B.Y.; Li, X.L.; Liu, C.W.; Wang, C.; Wang, F.; Chen, D.Y. Research on roof damage mechanism and control technology of gob-side entry retaining under close distance gob. *Eng. Fail. Anal.* **2022**, *138*, 106331. [CrossRef]

17. Li, X.L.; Chen, S.J.; Wang, S.; Zhao, M.; Liu, H. Study on in situ stress distribution law of the deep mine taking Linyi Mining area as an example. *Adv. Mater. Sci. Eng.* **2021**, *2021*, 5594181. [CrossRef]

18. Li, T.; Chen, G.B.; Qin, Z.C.; Li, Q.H.; Cao, B.; Liu, Y.L. The gob-side entry retaining with the high-water filling material in Xin'an Coal Mine. *Geomech. Eng.* **2020**, *22*, 541–552.

19. Xie, S.R.; Wu, X.Y.; Chen, D.D.; Sun, Y.H.; Zeng, J.C.; Zhang, Q.; Ji, C.W.; Cheng, Q.; Wang, E.; Ren, Y.X. Automatic roadway backfilling of caving gangue for cutting roofs by combined support on gob-side entry retaining with no-pillars: A case study. *Adv. Mater. Sci. Eng.* **2019**, *2019*, 8736103. [CrossRef]

20. Chang, Q.L.; Tang, W.J.; Xu, Y.; Zhou, H.Q. Research on the width of filling body in gob-side entry retaining with high-water materials. *Int. J. Min. Sci. Technol.* **2018**, *28*, 519–524. [CrossRef]

21. Du, Z.W.; Chen, S.J.; Ma, J.B.; Guo, Z.P.; Yin, D.W. Gob-side entry retaining involving bag filling material for support wall construction. *Sustainability* **2020**, *12*, 6353. [CrossRef]

22. Luan, H.J.; Jiang, Y.J.; Lin, H.L.; Wang, Y.H. A new thin seam backfill mining technology and its application. *Energies* **2017**, *10*, 2023. [CrossRef]

23. Li, F.X.; Yin, D.W.; Zhu, C.; Wang, F.; Jiang, N.; Zhang, Z. Effects of Kaolin addition on mechanical properties for cemented coal gangue-fly ash backfill under uniaxial loading. *Energies* **2021**, *14*, 3693. [CrossRef]

24. Li, H.; Zu, H.D.; Zhang, K.L.; Qian, J.F. Study on filling support design and ground stress monitoring scheme for gob-side entry retention by roof cutting and stress relief in high-gas thin coal seam. *Int. J. Environ. Res. Public Health* **2022**, *19*, 3913. [CrossRef] [PubMed]

25. Ma, Z.Q.; Zhang, D.Y.; Cao, Y.Q.; Yang, W.; Xu, B. Study of key technology of gob-side entry retention in a high gas outburst coal seam in the Karst Mountain Area. *Energies* **2022**, *15*, 4161. [CrossRef]

26. Qin, T.; Ren, K.; Jiang, C.; Duan, Y.W.; Liu, Z.; Wang, L. Distribution law of mining stress of the gob-side entry retaining in deep mining thin coal seam. *Adv. Civ. Eng.* **2021**, *2021*, 5589948. [CrossRef]

27. Tian, Z.J.; Zhang, Z.Z.; Deng, M.; Yan, S.; Bai, J.B. Gob-side entry retained with soft roof, floor, and seam in thin coal seams: A case study. *Sustainability* **2020**, *12*, 1197. [CrossRef]

28. He, M.C.; Gao, Y.B.; Yang, J.; Gong, W.L. An innovative approach for gob-side entry retaining in thick coal seam longwall mining. *Energies* **2017**, *10*, 1785. [CrossRef]

29. Li, X.L.; Chen, S.J.; Liu, S.M.; Li, Z.H. AE waveform characteristics of rock mass under uniaxial loading based on Hilbert-Huang transform. *J. Cent. South Univ.* **2021**, *28*, 1843–1856. [CrossRef]

30. Hu, J.Z.; He, M.C.; Wang, J.; Ma, Z.M.; Wang, Y.J.; Zhang, X.Y. Key parameters of roof cutting of gob-side entry retaining in a deep inclined thick coal seam with hard roof. *Energies* **2019**, *12*, 934. [CrossRef]

31. Elik, A.; Zelik, Y. Investigation of the efficiency of longwall top coal caving method applied by forming a face in horizontal thickness of the seam in steeply inclined thick coal seams by using a physical model. *Int. J. Rock. Mech. Min.* **2021**, *148*, 104917.

32. Liu, X.Y.; He, M.C.; Wang, J.; Ma, Z.M. Research on non-pillar coal mining for thick and hard conglomerate roof. *Energies* **2021**, *14*, 299. [CrossRef]

33. Guo, Z.C.; Li, S.G. Research and application of key technology of gob-side entry retaining in working face with hard roof. *Fresenius Environ. Bull.* **2022**, *31*, 5967–5972.

34. Qiu, L.M.; Zhu, Y.; Song, D.Z.; He, X.Q.; Wang, W.X.; Liu, Y.; Xiao, Y.Z.; Wei, M.H.; Yin, S.; Liu, Q. Study on the nonlinear characteristics of EMR and AE during coal splitting tests. *Minerals* **2022**, *12*, 108. [CrossRef]

35. Shen, J.C.; Zhang, Y. Theory and application of gob-side entry retaining in thick three-soft coal seam. *Geofluids* **2021**, *2021*, 6157174. [CrossRef]

36. Qi, F.Z.; Ma, Z.G.; Li, N.; Li, B.; Wang, Z.L.; Ma, W.X. Numerical analysis of the width design of a protective pillar in high-stress roadway: A case study. *Adv. Civ. Eng.* **2021**, *2021*, 5533364. [CrossRef]

37. Qiu, L.M.; Liu, Z.T.; Wang, E.Y.; He, X.Q.; Feng, J.J.; Li, B.L. Early-warning of rock burst in coal mine by low-frequency electromagnetic radiation. *Eng. Geol.* **2020**, *279*, 105755. [CrossRef]

38. Kong, X.G.; He, D.; Liu, X.F.; Wang, E.Y.; Li, S.G.; Liu, T.; Ji, P.F.; Deng, D.Y.; Yang, S.R. Strain characteristics and energy dissipation laws of gas-bearing coal during impact fracture process. *Energy* **2022**, *242*, 123028. [CrossRef]

39. Sun, Y.T.; Bi, R.Y.; Sun, J.B.; Zhang, J.F.; Taherdangkoo, R.; Huang, J.D.; Li, G.C. Stability of roadway along hard roof goaf by stress relief technique in deep mines: A theoretical, numerical and field study. *Geomech. Geophys. Geo-Energy Geo-Resour.* **2022**, *8*, 45. [CrossRef]

40. Das, A.J.; Mandal, P.K.; Bhattacharjee, R.; Tiwari, S.; Kushwaha, A.; Roy, L. Evaluation of stability of underground workings for exploitation of an inclined coal seam by the ubiquitous joint model. *Int. J. Rock. Mech. Min.* **2017**, *93*, 101–114. [CrossRef]

41. Sun, X.; Zhao, C.; Li, G.; Zhang, B.; Wang, J.; Cai, F. Physical model experiment and numerical analysis on innovative gob-side entry retaining with thick and hard roofs. *Arab. J. Geosci.* **2020**, *13*, 1245. [CrossRef]

42. Wang, Y.L.; Tang, J.X.; Dai, Z.Y.; Yi, T.; Li, X.Y. Flexible roadway protection technology in medium-thickness coal seam with large dip angle. *Energy Sources Part A-Recovery Util. Environ. Eff.* **2019**, *41*, 3085–3102. [CrossRef]

43. Lv, W.Y.; Guo, K.; Wu, Y.P.; Tan, Y.; Ding, K.; Li, B. Compression characteristics of local filling gangue in steeply dipping coal seam. *Energy Explor. Exploit.* **2022**, *40*, 1131–1150. [CrossRef]

44. Cao, W.X.; Liu, H.L.; Hang, Y.J.; Wang, H.Z.; Li, G.D. Similarity simulation on the movement characteristics of surrounding rock and floor stress distribution for large-dip coal seam. *Sensors* **2022**, *22*, 2761. [CrossRef]

45. Kong, X.G.; Li, S.G.; Wang, E.Y.; Wang, X.; Zhou, Y.X.; Ji, P.F.; Shuang, H.Q.; Li, S.R.; Wei, Z.Y. Experimental and numerical investigations on dynamic mechanical responses and failure process of gas-bearing coal under impact load. *Soil Dyn. Earthq. Eng.* **2021**, *142*, 106579. [CrossRef]

46. He, S.Q.; Song, D.Z.; He, X.Q.; Chen, J.Q.; Ren, T.; Li, Z.L.; Qiu, L.M. Coupled mechanism of compression and prying-induced rock burst in steeply inclined coal seams and principles for its prevention. *Tunn. Undergr. Sp. Technol.* **2020**, *98*, 103327. [CrossRef]

47. Wang, H.W.; Wu, Y.P.; Liu, M.F.; Jiao, J.Q.; Luo, S.H. Roof-breaking mechanism and stress-evolution characteristics in partial backfill mining of steeply inclined seams. *Geomat. Nat. Hazards Risk* **2020**, *11*, 2006–2035. [CrossRef]

48. Jiang, L.L.; Yang, Z.Q.; Li, G.W. Research on the reasonable coal pillar width and surrounding rock supporting optimization of gob-side entry under inclined seam condition. *Adv. Civ. Eng.* **2021**, *2021*, 7145821. [CrossRef]

49. Cui, F.; Dong, S.; Lai, X.P.; Chen, J.Q.; Jia, C.; Zhang, T.H. Study on the fracture law of inclined hard roof and surrounding rock control of mining roadway in longwall mining face. *Energies* **2020**, *13*, 5344. [CrossRef]